HHS Public Access

Author manuscript

Nat Med. Author manuscript; available in PMC 2019 January 23.

Published in final edited form as:

Nat Med. 2018 August ; 24(8): 1157–1166. doi:10.1038/s41591-018-0105-8.

Oncogenic hijacking of the stress response machinery in T cell acute lymphoblastic leukemia

Nikos Kourtis[1,*], **Charalampos Lazaris**[1,*], **Kathryn Hockemeyer**[1], **Juan Carlos Balandrán**[2], **Alejandra R. Jimenez**[2], **Jasper Mullenders**[1,8], **Yixiao Gong**[1], **Thomas Trimarchi**[1], **Kamala Bhatt**[1], **Hai Hu**[1], **Liza Shrestha**[3], **Alberto Ambesi-Impiombato**[4,9], **Michelle Kelliher**[5], **Elisabeth Paietta**[6], **Gabriela Chiosis**[3], **Monica L. Guzman**[2], **Adolfo A. Ferrando**[4], **Aristotelis Tsirigos**[1,7], and **Iannis Aifantis**[1]

[1]Department of Pathology and Laura and Isaac Perlmutter Cancer Center, NYU School of Medicine, New York, NY 10016, USA

[2]Haematology and Medical Oncology, Department of Medicine, Weill Cornell Medical College, New York, NY 10065, USA

[3]Program in Chemical Biology, Sloan Kettering Institute, New York, NY 10065, USA

[4]Institute for Cancer Genetics, Department of Pathology and Department of Pediatrics, Columbia University, New York, NY 10032, USA

[5]Department of Molecular, Cell and Cancer Biology, University of Massachusetts Medical School, Worcester, MA 01605, USA

[6]Montefiore Medical Center, New York, NY 10466, USA

[7]Applied Bioinformatics Laboratories, NYU School of Medicine, New York, NY 10016, USA

Abstract

Cellular transformation is accompanied by extensive re-wiring of many biological processes leading to augmented levels of distinct types of cellular stress, including proteotoxic stress. Cancer cells critically depend on stress-relief pathways for their survival. However, the mechanisms underlying the transcriptional initiation and maintenance of the oncogenic stress response remain elusive. Here, we show that the expression of heat shock transcription factor 1 (*HSF1*) and the downstream mediators of the heat shock response is transcriptionally upregulated in T-cell acute

Correspondence should be addressed to I.A (Iannis.Aifantis@nyumc.org) or N.K. (Nikolaos.Kourtis@nyumc.org).

[8]Present address: Hubrecht Institute, Royal Netherlands Academy of Arts and Sciences (KNAW) and University Medical Centre (UMC) Utrecht, 3584 CT Utrecht, the Netherlands

[9]Present address: PsychoGenics Inc., Tarrytown, New York, NY 10591, USA

[*]These authors contributed equally to this work.

Author contributions. N.K. and I.A. designed the experiments and wrote the manuscript. N.K. performed most of the experiments. C.L. designed and performed bioinformatics analysis of genome-wide data. K.H., J.C.B, A.R.J., J.M. and T.T. performed experiments. Y.G. performed RNA-seq analysis. K.B. and H.H maintained the mouse colonies. L.S. provided molecular chaperones inhibitors. M.K. provided Tal1 cells. A.A.-I., E.P. and A.A.F. provided T-ALL patient expression data and patient samples. G.C. and M.L.G. provided molecular chaperones inhibitors and ideas. A.T. designed and performed bioinformatics analysis of genome-wide data and contributed ideas.

Competing financial interests statement. The authors declare that they have no competing financial interests.

lymphoblastic leukemia (T-ALL). *Hsf1* ablation suppresses the growth of human T-ALL and eradicates leukemia in mouse models of T-ALL, while sparing normal hematopoiesis. HSF1 drives a compact transcriptional program and among the direct HSF1 targets, specific chaperones and co-chaperones mediate its critical role in T-ALL. Notably, we demonstrate that the central T-ALL oncogene NOTCH1 hijacks the cellular stress response machinery by inducing the expression of *HSF1* and its downstream effectors. The NOTCH1 signaling status controls the levels of chaperone/co-chaperone complexes and predicts the response of T-ALL patient samples to HSP90 inhibition. Our data demonstrate an integral crosstalk between mediators of oncogene and non-oncogene addiction and reveal critical nodes of the heat shock response pathway that can be targeted therapeutically.

Multiple oncogenic insults converge on the transcriptional upregulation of anabolic pathways. Runaway cancer cell growth overwhelms the cellular proteome homeostasis and elicits the heat shock response to counter proteotoxic stress[1–4]. Stress alleviation is orchestrated by HSF1 and mediated by induced heat shock proteins (HSPs)[5–8]. The altered dependencies of cancer cells on stress response pathways have been proposed as an attractive therapeutic opportunity[9,10].

Despite the importance of proteotoxic stress relief mechanisms in cancer, the regulation of HSF1 by oncogenic signaling pathways remains elusive[6,11]. In experiments where HSF1 is activated by external stress, protein-protein interactions and extensive post-translational modifications have been shown to regulate HSF1 activity[8,11]. However, the molecular pathways responsible for the transcriptional initiation and maintenance of the heat shock response pathway in cancer are poorly understood[6,8,11]. Moreover, a comprehensive characterization of the direct effectors of HSF1 and the crosstalk of HSF1 with other transcription factors in disease conditions are missing[6,8,11,12].

To gain insight into the molecular basis of heat shock response regulation in cancer, we focused on T-ALL as a disease model. Although the growth-promoting pathways driven by aberrantly activated oncogenes in T-ALL have been elucidated[13–15], the regulation of supportive mechanisms (non-oncogenic *per se*) in acute leukemia cells has not been addressed. Current intensive chemotherapy regimens to pediatric and adult T-ALL patients come at the cost of serious side effects while a significant percentage of patients experience relapse, reinforcing the need to understand the altered dependencies of leukemia cells and target novel pathways to which tumor cells are specifically addicted.

RESULTS

Expression of *HSF1* and the downstream heat shock response are induced in human T-ALL

A plethora of post-translational modifications are critical for the stability and activation of HSF1[11,16–23]. However, the transcriptional regulation of *HSF1* expression in cancer remains unknown[6,11]. Gene expression profiling of pediatric T-ALL[24] samples revealed significant upregulation of *HSF1* expression compared to thymocyte subsets purified from healthy individuals (Fig. 1a). In addition, total HSF1 protein levels and phosphorylated on Ser326

HSF1, a modification critical for HSF1 activation[25], were significantly higher in primary T-ALL patient samples and T-ALL cell lines (the CUTLL1 line is shown as a representative example[26]) compared to normal T cells (Fig. 1b). We next examined whether elevated expression of *HSF1* may induce transcriptionally the heat shock response pathway. To address this possibility, we surveyed the expression of classic gene-members of the heat shock response pathway[27] in T-ALL primary patient samples. We found that well-characterized HSF1 targets such as *HSP90AB1*, *HSPA8* (*HSP70*) and *HSPH1* exhibit significantly higher expression in T-ALL samples (Fig. 1c and Supplementary Fig. 1a). In addition, using a second independent patient dataset, we observed significantly higher expression of *HSF1* and classic HSF1 targets in T-ALL samples compared to normal T-cells (Supplementary Fig. 1b).

HSF1 is essential for disease progression in animal models of T-ALL

The significant upregulation of expression of *HSF1* and classic HSF1 targets in T-ALL patient specimens suggested a potential involvement of this stress response program in the pathogenesis of acute leukemia. To test this hypothesis, we initially knocked down *HSF1* in human T-ALL cell lines using previously validated short hairpin RNAs (shRNA)[1,21]. *HSF1* depletion led to increased rates of apoptosis (Fig. 1d), defective proteostasis as exemplified by upregulation of ER stress markers (Supplementary Fig. 1c) and strongly affected growth of leukemic cells (Fig. 1e and Supplementary Fig. 1d, e). These experiments suggested that T-ALL cells are addicted to HSF1 function.

To establish conclusively whether HSF1 is required for T-ALL progression *in vivo*, we generated and studied a NOTCH1-induced T-ALL animal model (Supplementary Fig. 2a). We utilized this model since NOTCH1 pathway is hyper-active in the vast majority of T-ALL cases[13]. We used an inducible Cre recombinase model to delete *Hsf1* after disease establishment. Bone marrow progenitor cells derived from $Hsf1^{f/f}$Mx1-Cre^{+} mice or littermate control mice ($Hsf1^{+/+}$Mx1-Cre^{+}) were retrovirally transduced with an “active” NOTCH1 mutant (NOTCH1-ΔE-IRES-GFP)[28] and transplanted into lethally irradiated wild type recipients. Upon disease establishment, we genetically ablated *Hsf1* (Supplementary Fig. 2b) and examined leukemia burden and disease progression. *Hsf1* deletion led to a striking reduction of leukemic cell numbers and infiltration in all tissues surveyed (Fig. 2a–c and Supplementary Fig. 2c). Given the striking reduction in leukemia burden upon *Hsf1* deletion, we assessed animal survival. We found that, compared to littermate control mice, survival of *Hsf1*-depleted animals was dramatically extended (Fig. 2d). Notably, there was no fatality recorded in the $Hsf1^{f/f}$Mx1-Cre^{+} animals group for a period longer than a year, suggesting an absolute addiction of T-ALL cells on HSF1 function.

The *in vivo* NOTCH1-ΔE T-ALL model survival data suggested that *Hsf1* loss could directly impact leukemia initiating cells (LIC) function, as no relapse incidence was recorded. We have previously characterized LICs in this model of T-ALL and shown that Myc protein abundance is a *bona fide* LIC biomarker. This LIC subset corresponds to a small fraction of the overall T-ALL cell population and is characterized by a specific cell surface expression signature[29]. To test the role of Hsf1-orchestrated stress response in T-ALL LICs we studied the Myc^{+} LIC transcriptome and compared it to Myc^{neg} cells that have no LIC capacity. We

found that Myc^{+} LICs are characterized by high expression of a number of Hsf1 target genes (Fig. 2e). Together with our *in vivo* T-ALL remission data, these findings suggest that T-ALL cells are addicted to Hsf1 function and LICs are characterized by an enhanced Hsf1-driven stress response.

To examine the effect of *Hsf1* silencing in an additional T-ALL model (not driven by NOTCH1), we used T-ALL cells derived from a Tal1 mouse model. In this model, Tal1 is the initiating oncogenic trigger[30]. *Hsf1* knockdown strongly affected the survival of *Tal1*-overexpressing leukemic cells *in vitro* (Supplementary Fig. 2d, e). To test a requirement for Hsf1 in Tal1-driven leukemia progression *in vivo*, we infected primary mouse Tal-1-driven T-ALL leukemia cells[31] with lentiviruses encoding shRNAs to *Hsf1* (or Renilla Luciferase, as a control) and transplanted the infected cells to syngeneic recipients. Silencing of *Hsf1* resulted in striking reduction of peripheral T-ALL cells (characterized by co-expression of CD4 and CD8; Supplementary Fig. 2f) and significant increased overall animal survival (Supplementary Fig. 2g).

Hsf1 ablation does not affect normal hematopoiesis *in vivo*

It was previously shown that Hsf1 expression is dispensable for survival of mice under normal growth conditions[32]. To investigate possible effects of *Hsf1* loss on cellular fitness specifically in the hematopoietic system, we undertook competitive bone marrow transplantation assays (using a 1:1 mixture of *Hsf1*-expressing and non-expressing bone marrow stem and progenitor cells). We found that *Hsf1* depleted hematopoietic stem and progenitor cells (HSPCs) reconstituted recipient mice bone marrow efficiently (Fig. 2f, g) and were able to generate all blood lineages (data not shown), including T-cells in the same proportions as their wild type counterparts (Supplementary Fig. 3a, b). Moreover, *Hsf1* deletion specifically in the hematopoietic system of adult mice did not affect steady-state hematopoiesis or the lymphoid compartment (Supplementary Fig. 3c). These experiments demonstrate that Hsf1 is specifically required for the viability of “stressed” leukemic cells but is dispensable for hematopoietic stem cell function and normal T-cell development, suggesting a potential therapeutic window for future HSF1 targeting for leukemia treatment.

Genomic mapping of the HSF1-regulated stress response in acute leukemia

Our laboratory and others have previously shown that HSF1 demonstrates cancer-type and mutation-specific genome occupancy patterns[2,21]. To connect direct HSF1 gene targets to HSF1 function in leukemia, we sought to characterize the human T-ALL HSF1 transcriptional program. Chromatin immunoprecipitation followed by sequencing (ChIP-seq) studies in human T-ALL cells (CUTLL1) mapped the HSF1 chromatin occupancy signature. We found that the majority of HSF1 binding peaks (~75%) are located at transcription start sites (TSS) of putative target genes (Supplementary Fig. 4a), suggesting a HSF1 preference for promoter regions. Bioinformatics analysis of these promoter regions revealed a strong enrichment for consensus HSF1 binding elements[33] (Supplementary Fig. 4b; $P<10^{-29}$). In addition, gene ontology analysis showed enrichment for protein folding functions (Supplementary Fig. 4c; $P<10^{-6}$). Based on these ChIP-seq results, we defined a TSS-centric HSF1 gene target signature. We found that, in contrast to broad HSF1 genome occupancy in solid tumors[2,21] and tumor stroma[34], HSF1 occupies the promoters of a small

number (less than 70) of genes in T-ALL. Examination of expression of the genes bound by HSF1 on their promoters demonstrated contrasting patterns between T-ALL patient samples and control thymocyte subsets (Fig. 3a). To further identify direct HSF1 transcriptional targets, we combined our ChIP-seq analysis with RNA sequencing (RNA-seq) upon brief silencing of *HSF1* in human T-ALL cells (Supplementary Fig. 4d). This analysis allowed us to define a group of genes that comprise the "direct HSF1 gene signature" in this cancer type (Supplementary Table 1). We then asked whether these genes are differentially expressed in primary human T-ALL. We found that positively regulated HSF1 targets are upregulated in T-ALL samples (when compared to physiological thymocyte subsets) and negatively regulated targets are downregulated (Supplementary Fig. 4e). Thus, this combinatorial analysis uncovered direct HSF1 targets in acute leukemia and showed that the T-ALL HSF1 gene signature is distinct from the signatures previously defined in solid tumors and tumor stroma.

Functional mapping of the HSF1-regulated stress response in acute leukemia

An emerging question based on this definition of HSF1 gene signature is which of these targets mediate the HSF1 phenotype and are essential for T-ALL cell growth. A plausible scenario, pertinent to the strong requirement of HSF1 for T-ALL survival, involves the coordinated function of several direct HSF1 targets. To test this hypothesis, we surveyed all the HSF1 positively regulated targets for their ability to mimic the effect of *HSF1* knockdown on leukemia cell growth, using a targeted RNAi screen. We found that silencing of a number of single HSF1 direct targets (10 out of 23) was sufficient to suppress the growth of human T-ALL cells (Figure 3b, Supplementary Fig. 4f). Interestingly, all these "essential" targets belong to the HSP90/HSP70 chaperone and co-chaperone interaction network[35] (Fig. 3c). Overexpression of *HSP90AB1*, a key molecular chaperone that nucleates this functional network, was not sufficient to rescue the effect of *HSF1* knockdown on T-ALL survival (Supplementary Fig. 4g), suggesting non-overlapping functions of the various HSF1 targets. HSF1 ChIP-seq analysis in a second human T-ALL cell line further supported these findings as it showed that common gene targets between the two cell lines include the "essential" HSF1 targets identified in our screen (Fig. 3d). Together, our findings functionally characterize the HSF1 targets in human leukemia and indicate the presence of a well-defined functional HSF1 transcriptional program in acute T-cell leukemia.

NOTCH1 hijacks the stress response machinery

The heat shock response pathway was described more than 50 years ago and has been implicated in the pathogenesis of diseases as diverse as neurodegeneration and cancer. However, the transcriptional trigger of the pathway remains elusive. Based on our findings showing upregulation of HSF1 mRNA expression in T-ALL, we sought to elucidate the mechanism underlying HSF1 transcriptional upregulation in this type of leukemia. We hypothesized that oncogenes may include anabolism-supportive pathways in their altered transcriptional program. Aberrant constitutively active NOTCH1 signaling is a defining feature of the vast majority (>90%) of human T-ALL cases[36,37]. NOTCH1 ChIP-seq analysis in human T-ALL cells[26,38], revealed binding of NOTCH1 on both HSF1 TSS and gene body (Fig. 4a). The HSF1 promoter was also occupied by RNA polymerase II (Pol II) and marked by the presence of H3K4me3 (Fig. 4a), in agreement with the active status of

the locus. NOTCH1 binding on the HSF1 promoter was further confirmed by ChIP-qPCR analysis (Supplementary Fig. 5a). Moreover, NOTCH1 binding on the HSF1 promoter was detected in an additional T-ALL line (JURKAT; Supplementary Fig. 5b). By contrast, we did not detect binding of NOTCH1 on the HSF1 promoter in normal HSPCs, even upon heat shock treatment, suggesting that oncogenic stress differs both in type and intensity from this of the classic heat shock (Supplementary Fig. 5c). Thus, our data directly link heat shock response to an oncogenic transcription factor and suggest oncogenic hijacking of the non-oncogenic stress response.

Upon exposure to heat stress, HSF1 drives the expression of heat-inducible genes by increasing RNA Pol II release from promoter-proximal pause[39,40]. However, the transcriptional regulation of HSF1 targets in cancer is unknown. Intriguingly, we observed a broad co-occupancy of HSF1 and NOTCH1 on the promoters of a large number of HSF1 targets (Fig. 4b; 48 out of 57 HSF1 targets, $P=2.2 \times 10^{-16}$, Chi-squared test). Bioinformatics analysis revealed distinct binding motifs for these transcription factors on the promoters of stress response genes (Supplementary Fig. 5d). Occupancy of the promoters of *HSF1* and heat shock proteins coding genes by NOTCH1 indicates a potential involvement of this oncogene in transcriptional control of the heat shock response pathway. To test this hypothesis, we initially monitored the expression of *HSF1* upon inhibition of NOTCH1 pathway. Treatment of T-ALL cells with γ-secretase inhibitor (γSI)[41], to block NOTCH1 cleavage and pathway activation, resulted in significant downregulation of HSF1 expression at both mRNA and protein level (Fig. 4c and Supplementary Fig. 6a). We observed similar effects upon treatment of multiple T-ALL cell lines with γSI (Supplementary Fig. 6b). Notably, NOTCH1 signaling inhibition had no effect on *HSF1* expression in the leukemic cell line LOUCY[42] that is characterized by the absence of *NOTCH1* expression (Supplementary Fig. 6b). In addition, γSI treatment reduced *HSF1* expression in primary T-ALL patient samples (Supplementary Fig. 6c). To further examine the correlation between *HSF1* expression and NOTCH1 pathway activity, we analyzed a T-ALL patient dataset and categorized patients into 20% highest and 20% lowest *NOTCH1* expressing. Consistent with our model suggesting regulation of the heat shock response by NOTCH1, we found that high *NOTCH1* expressing patient samples also expressed the highest levels of *HSF1* and heat shock response genes (Supplementary Fig. 6d). By contrast, samples expressing low *NOTCH1* levels were also characterized by low expression of *HSF1* and heat shock response genes (Supplementary Fig. 6d). Interestingly, subcellular fractionation analysis of primary T-ALL patient samples (maintained on the bone marrow-derived stromal cell line OP9 that expresses the Notch ligand Delta-like 1 (DLL1)[43]) revealed variability in the levels of nuclear NOTCH1. In line with our model, patient samples characterized by high nuclear NOTCH1 protein levels also expressed higher levels of HSF1 and stress proteins, compared to samples expressing low or no nuclear NOTCH1 (Fig. 4d). In addition, patient samples characterized by high expression of stress response mediators showed increased sensitivity to *HSF1* knockdown (Supplementary Fig. 6e).

We then assessed the expression of HSF1 targets whose promoters were also occupied by NOTCH1, upon NOTCH1 pathway inhibition. We found that, similar to *HSF1* knockdown, NOTCH1 inhibition resulted in reduction of expression of HSF1 targets (Fig. 4e). To further profile nascent RNAs during NOTCH1 signaling recovery after γSI treatment, we

performed global-run-on sequencing (GRO-seq)[44]. We observed increased transcriptional activity for HSF1 and HSF1 targets during recovery from NOTCH1 signaling inhibition (Supplementary Fig. 6f). What is the functional significance of NOTCH1-HSF1 co-occupancy on the promoters of stress response genes? To address this question, we knocked down *HSF1* (using shRNAs) and also inhibited the NOTCH1 pathway activation (using γSI). We observed cooperation in the reduction of expression of HSF1 target genes, including the chaperones and co-chaperones mediating the HSF1 effect on T-ALL survival (Fig. 4f). To investigate a potential direct interaction between NOTCH1 and HSF1, we characterized the nuclear NOTCH1 interactome in T-ALL and HEK293T cells, by mass-spectrometry. Although we detected the majority of known interactors of NOTCH1, we did not identify interaction with HSF1 (Supplementary Table 2), in agreement with a previous report characterizing the NOTCH1 interactome in T-ALL[45]. When we assessed the expression of *HSF1* and heat shock response targets across T-ALL lines, we found that leukemic cells characterized by *NOTCH1* expression had significantly higher levels of the stress signature, compared to leukemic cells not expressing *NOTCH1* (Supplementary Fig. 7a). Cell cycle analysis revealed similar kinetics among these cell lines (Supplementary Fig. 7b), excluding the possibility of the stress response being a mere reflection of the cell cycle status. Finally, to investigate whether NOTCH1 pathway activation is sufficient to induce the heat shock response pathway in a non-transformed context, we expressed a constitutively cleaved in a ligand-independent manner, form of NOTCH1 (ΔE mutant) in hematopoietic stem and progenitor cells (HSPCs, Lineage^{neg}c-Kit^{+}Sca-1^{+}) isolated from mouse bone marrow. We found that NOTCH1 pathway activation rapidly and significantly increased the expression of both *Hsf1* and several heat shock genes coding direct Hsf1 targets (Fig. 4g). Simultaneous expression of Notch1-ΔE and silencing of *Hsf1* suppressed the effect of NOTCH1 on *Hsf1* and stress response genes expression (Fig. 4g).

Finally, to test whether the NOTCH1-heat shock response axis is active in other blood malignancies, we tested distinct types of leukemia, including acute myeloid leukemia (AML) and chronic lymphocytic leukemia (CLL)[46]. We chose CLL as, similar to T-ALL, it is associated with oncogenic NOTCH1 mutations[47,48]. On the other hand, we have previously shown that the Notch pathway acts as tumor suppressor in AML[49]. Unlike T-ALL, we did not observe transcriptional upregulation of *HSF1* in AML or CLL patient samples (Supplementary Fig. 7c). We investigated whether this is the result of differential NOTCH1 genome occupancy patterns compared to T-ALL. We found that in CLL, where NOTCH1 has an oncogenic role[50], it does not occupy the promoters of HSF1 or its target genes (Supplementary Fig. 7d). Our findings, in their totality, demonstrate that in T-ALL, NOTCH1 hijacks the heat shock response machinery at the transcriptional level and raise the possibility that distinct tumor-specific transcription factors may regulate the proteotoxic stress relief machinery in a cancer type-specific way.

NOTCH1 regulates the functional T-ALL chaperome

Previous studies have shown that in the presence of oncogenic stress, heat shock proteins participate in a large functional and physical network nucleated by HSP90 and HSP70 chaperones, recently termed the “epichaperome”[51,52]. Based on our findings demonstrating transcriptional regulation of the heat shock response machinery by NOTCH1, we

hypothesized that this oncogene might directly regulate the epichaperome in T-ALL. To test this hypothesis, we initially examined whether an intact epichaperome is critical for T-ALL. In line with recent findings describing the effect of HSP90 inhibition on T-ALL cell lines viability[53], we found that pharmacologic HSP90 and HSP70 inhibition[51,54] significantly affected the growth of human T-ALL *in vitro*, leading to cell cycle arrest and increased apoptosis (Supplementary Fig. 8a–d). To examine the role of epichaperome perturbation in T-ALL *in vivo*, we treated the previously introduced NOTCH1-inducible T-ALL animal model with the HSP90 inhibitor PU-H71. HSP90 inhibition strongly reduced the leukemic burden (Supplementary Fig. 8e, f) and significantly extended the animal lifespan (Fig. 5a). These findings suggest that T-ALL is addicted to a functional network of chaperones and co-chaperones orchestrated by NOTCH1 and HSF1.

To further investigate the potential involvement of NOTCH1 signaling in epichaperome regulation, we monitored the levels of epichaperome upon treatment of T-ALL with NOTCH1 inhibitors (γSI). Using previously established chemical biology tools[52,55,56], we found that NOTCH1 pathway inhibition significantly reduced the levels of cellular epichaperome (Fig. 5b, Supplementary Fig. 9a). By contrast, γSI treatment had no effect on the epichaperome levels in LOUCY T-ALL cells that express no nuclear NOTCH1 (Fig. 5b, Supplementary Fig. 9a). Furthermore, we investigated whether activation of NOTCH1 signaling in untransformed cells affects epichaperome formation. We found that, active NOTCH1 induced epichaperome formation in mouse HSPCs (Supplementary Fig. 9b).

Previous studies have shown that the binding affinity of HSP90 for small molecule inhibitors and the cancer cell sensitivity to HSP90 inhibition dramatically increase when this molecular chaperone participates in multi-chaperone complexes[51,52,55]. Therefore, we assessed the effect of epichaperome levels reduction upon γSI treatment, on HSP90 inhibition outcome in T-ALL. We found that γSI pre-treatment suppressed the effect of PU-H71 on T-ALL survival and growth (Fig. 5c). However, γSI pre-treatment had no effect on PU-H71 efficacy in LOUCY T-ALL cells (Fig. 5c). Moreover, γSI pre-treatment of patient T-ALL samples significantly reduced cell death triggered by PU-H71 treatment (Supplementary Fig. 9c). Given the research efforts to identify optimal drug combinations in cancer, our findings suggest that drugs targeting the NOTCH1 signaling pathway may impede the efficiency of molecular chaperones inhibitors, providing a warning for future combinatorial treatments.

NOTCH1 activation predicts response to chaperome-targeted therapy

These studies suggest that high levels of expression of nuclear NOTCH1, and consequently high levels of epichaperome, provide an attractive biomarker for response to HSP90 inhibitors. Given the variability in the levels of nuclear NOTCH1 observed in T-ALL patient samples (Fig. 4d), we monitored the epichaperome levels in primary T-ALL patient samples. Intriguingly, patient samples expressing high levels of nuclear NOTCH1 (patients 6–10), expressed higher levels of epichaperome compared to those with low nuclear NOTCH1 expression (patients 1–5; Fig. 6a, Supplementary Fig. 10a, b).

Finally, we tested whether patient nuclear NOTCH1 levels can predict the response to HSP90 inhibition. We found that patient samples expressing high levels of nuclear NOTCH1 and high levels of epichaperome (patients 6–10) were significantly more sensitive to PU-

H71 treatment compared to T-ALL with low nuclear NOTCH1 (patients 1–5; Fig. 6b). Our findings, in their totality, suggest that the NOTCH1 signaling pathway regulates the epichaperome levels and impacts the outcome of HSP90 inhibition on leukemia survival.

DISCUSSION

Our studies implicate HSF1 as a dominant orchestrator in acute leukemia and provide a number of key novel insights into the role and regulation of the heat shock response pathway, a universal response to which virtually all cancers are addicted. So far, and based primarily on studies where HSF1 is activated by heat, HSF1 has been shown to be regulated by numerous protein-protein interactions and extensive post-translational modifications. Our findings suggest that in T-ALL, the oncogene NOTCH1, a defining cancer trigger in this disease, hijacks the heat shock response pathway through transcriptional regulation of HSF1. Additionally, we provide evidence for the presence of a previously unsuspected crosstalk between mediators of oncogene and non-oncogene addiction. Specifically, we show interplay between an oncogene (NOTCH1) and HSF1 on the control of expression of critical effectors of the oncogenic stress relief machinery. Our data mechanistically explain previous observations in the stress response field suggesting that transcription factors, other than HSF1, may regulate HSF1 target gene expression in disease[11,12]. What is the molecular basis of this interplay? NOTCH1 promotes leukemia cell growth via direct transcriptional upregulation of anabolic pathways, including overactive transcription, ribosome biosynthesis and protein translation[26,57]. We propose that, due to increased anabolism, the folding demands of leukemic cells are amplified and parallel activation of the heat shock response pathway might be vital for proteostasis maintenance (Fig. 6c). Characterization of the proteostasis machinery clientele in T-ALL will reveal crucial mediators of leukemogenesis. Interestingly, intracellular Notch1 itself has been recently proposed to be a novel client of HSP90[58].

Why oncogene-mediated transcriptional hijacking of the stress response pathway may be required in T-ALL (and possibly in other cancer types)? We propose that accumulation of a critical number of HSF1 molecules is necessary for the initiation of the HSF1 cancer-specific transcriptional program. Work from our group and others has shown that this critical HSF1 protein abundance can be achieved through mechanisms like mutation/silencing of E3 ligases or upregulation of oncogenic pathways that post-translationally modify critical for stability residues, and these mechanisms can be cancer-type specific[21,59]. Our data suggest an additional -but not mutually exclusive- mechanism, that of oncogene-mediated transcriptional upregulation of *HSF1* and HSF1-targets expression. Further investigation will reveal whether NOTCH1 regulates the heat shock response pathway in other types of cancer or this crosstalk is mediated by tumor specific oncogenes.

To date, there are no approved drugs targeting the NOTCH1 pathway, despite the development of a number of promising experimental compounds including γ-secretase. Our findings suggest that the heat shock response pathway may provide an alternative option for targeting cancers driven by NOTCH1, while sparing normal cells. Interestingly, our studies suggest that HSF1 targeting compromises the viability of cancer-initiating cells, an exciting finding given the potential role of such populations in disease relapse after treatment. In

addition to the preclinical and early clinical promise of HSP90 and HSP70 inhibitors [52,54], our findings uncover a battery of chaperones and co-chaperones critical for T-ALL survival. We anticipate that these oncogenic stress relief mediators could serve as novel intervention targets in an effort to battle leukemia and other types of cancer that are addicted to the heat shock response pathway for survival. Given that it is unlikely that every single chaperone and co-chaperone encoded by the genome will participate in the chaperome network and will be critical for a particular tumor type, an integrative approach similar to the one followed in our study will uncover tumor-specific altered dependencies on the chaperome machinery.

Currently, there is insufficient stratification of patients enrolled in trials targeting molecular chaperones, including HSP90[60]. Our findings suggest that the status of NOTCH1 signaling may serve as a biomarker for the clinical outcome of therapeutic interventions targeting the stress response cellular machinery. Altered dependency of cancer cells on non-oncogenic stress-relief mechanisms has emerged as a novel anti-cancer therapy class. If its preclinical promise is to be realized, it is imperative that we decipher the regulation of this cancer anabolism-supportive pathway. Our study provides one of the first in depth characterizations of the mechanism of regulation and action of the stress response in cancer.

METHODS

Animals

The *Hsf1* conditional mouse models, as well as the corresponding genotyping strategy, have been described previously[61]. Mx1-Cre mice and C57BL/6 mice (6–8 weeks old) were obtained from Jackson Laboratory. To induce deletion by Mx1-Cre, mice received four intraperitoneal injections of poly(I:C) (10 ug/g, GE Healthcare), administered every other day. To determine the effect of *Hsf1* silencing on the survival of the Tal1 model, *Tal1* T-ALL cells were infected with lentiviruses expressing Renilla luciferase or *Hsf*1 specific shRNAs. Selected mouse leukemic cells were transplanted into syngeneic recipient mice as described previously[31,62] and disease development was monitored. All animal experiments were performed in accordance with protocols approved by the New York University Institutional Animal Care and Use Committee (IACUC).

Bone marrow cells transduction and transplantation

For analysis of leukemia progression, c-kit+ hematopoietic stem and progenitor cells were enriched from bone marrow by magnetic selection (STEMCELL Technologies) using an antibody against CD117 (c-kit) and cultured in the presence of 50 ng/ml Flt3 ligand, 50 ng/ml SCF, 10 ng/ml IL-3 and 10 ng ml IL-6. 24 and 48 h after enrichment, c-kit$^+$ cells were infected with concentrated retrovirus expressing NOTCH1-ΔE-IRES-GFP$^+$ or control vector. Transduction efficiency was determined by reporter fluorescence monitoring over a total period of 4 days. For induction of T-ALL, irradiated mice (two rounds of 550 rads) received 5×10^4 GFP$^+$ cells, together with 5×10^5 bone marrow mononuclear cells (wild type) for hemogenic support, via retro-orbital injection. The Mantel-Cox test was used for the analysis of survival data. No randomization or blinding method was used in these animal studies.

Competitive transplantation of bone marrow

Bone marrow was isolated from and *Hsf1*$^{f/f}$*Mx1-Cre*$^{+}$ (CD45.2^{+}) donor mice and support *Hsf1*$^{+/+}$*Mx1-Cre*$^{+}$ (CD45.1^{+}) donor mice. Donor cells (1×10^6 per mouse) were mixed at a ratio 1:1 with support bone marrow cells and transplanted via retro-orbital injection into lethally irradiated (550 rads, twice) CD45.1^{+} recipient mice. Two weeks after transplantation, mice were injected with poly(I:C) to induce deletion by Mx1-Cre (see above). Chimerism was monitored by flow cytometry of peripheral blood (with anti-CD45.1 (A20; BD Bioscience) and anti-CD45.2 (104; BD Bioscience)) at 4-week intervals after transplantation for 20 weeks, at which time mice were sacrificed for assessment of chimerism in bone marrow and spleen.

In vivo animal treatment

For inhibition of HSP90, mice were treated with intraperitoneal injections 75mg/kg PU-H71 (Selleckhem) or PBS, 3 times per week. Treatment was initiated 2 weeks after transplantation, upon detection of ~10% leukemic (GFP^{+}) cells in the peripheral blood

Cell culture and primary cell samples

The human cell lines CUTLL1[26] and P12, CEM and KOPTK1 were cultured in RPMI 1640 medium supplemented with 20% FBS, penicillin and streptomycin. The mouse T-ALL line Tal1 was cultured in RPMI 1640 medium supplemented with 10% FBS and penicillin and streptomycin. All cell lines were tested for presence of mycoplasma and only mycoplasma-free lines were used for these studies. T-ALL patient samples were maintained on the bone marrow-derived stromal cell line OP9 expressing the Notch ligand Delta-like 1 (DLL1)[43]. Primary T-ALL patient samples and blood from healthy donors were collected at Columbia Presbyterian Hospital with informed consent, under the supervision of the Columbia University Medical Center Institutional Review Board.

In vitro drug treatment and cell growth and cell cycle analysis

γ-secretase inhibitor (γSI, Compound E (Alexis Biochemicals)) was used at 1μM for the indicated periods. HSP90 and HSP70 inhibitors (PU-H71 and YK222 respectively) were used at 500 nM for the indicated periods. PU-H71 and YK222 were synthesized using previously reported procedures[52,63]. Apoptosis was studied by quantification of annexin V staining using the BD Biosciences kit and flow cytometry according to standard protocols provided by the manufacturer. For the cell cycle analysis, the Click-iT Plus EdU proliferation kit was used according to standard protocol provide by the manufacturer.

Epichaperome abundance measurement using PU-FITC flow cytometry assay

The PU-FITC assay was performed as previously described[52,55,56]. HL-60 and MV4–11 were used as negative and positive controls respectively for epichaperome abundance. The control derivative PU-FITC9 was used as a negative control. The mean fluorescence intensity (MFI) of PU-FITC in viable cells (DAPI negative) was evaluated by flow cytometry.

Antibodies, reagents, kits and virus production

Antibodies against the following proteins were used: polyclonal rabbit HSF1 (Cell Signaling, 4356), monoclonal rabbit pS326 HSF1 (Abcam, 76076), monoclonal mouse HSP90AB1 (GeneTex, 84342), monoclonal rabbit HSPA8 (Cell signaling, 8444), monoclonal rabbit NOTCH1 (Cell Signaling, 4147), monoclonal mouse Actin (Millipore, MAB1501) and polyclonal goat Lamin A (Santa Cruz biotechnology, sc-6214). The shRNAs used against HSF1 and HSF1 positively regulated targets are described in Supplementary Table 3. To generate virus, we transfected HEK293T cells with a plasmid (pLKO.1) expressing the shRNA of interest and lentiviral packaging plasmids. Viral supernatant was collected over a period of 72 h and used for the transduction of T-ALL cells. For survival assays, the cells were infected twice and selected with puromycin starting 2 days after viral infection. For RNA-seq experiments and to avoid the effects of apoptosis due to *HSF1* knockdown, infection conditions were optimized to reach ~90% transduction efficiency and RNA was collected 48 h after infection.

Quantitative real-time PCR

For mRNA quantification, total RNA was isolated from one million cells for each condition and replicate using the RNeasy Plus Mini Kit (QIAGEN). RNA was quantified by absorbance at A_{260nm} and 1 μg of total RNA used for cDNA synthesis using Superscript III first strand synthesis kit (Invitrogen). Real-time PCR reactions were carried out using SYBR Green Master Mix (Roche) and run with a Lightcycler 480 II (Roche). The following primer sequences were used for cDNA quantification: human *HSF1* for 5′-CCGTGTCCTGTGGTTTGGTT-3′, rev 5′-CTGTCTTGTCCGTCCATCCA-3′; human *HSP90AA1* for 5′-AAAGGCGAACGTCTCAACC-3′, rev 5′-GGTCCTGTGCGGTCACTTAG-3′; human *HSP90AB1* for 5′-AAAGGCGAACGTCTCAACC-3′, rev 5′-GGTCCTGTGCGGTCACTTAG-3′; human *HSPD1* for 5′-TTGACTGCCACAACCTGAAG-3′, rev 5′-CACCGTAAGCCTTTGGTCAT-3′; human *HSPE1* for 5′-TGCCTCCATATTCTGGGAGA-3′, rev 5′-AGTAGTCGCTGTTGGATCGG-3′; human *CHOP* for 5′-AGAACCAGGAAACGGAAACAGA-3′, rev 5′-TCTCCTTCATGCGCTGCTTT-3′; human *HSPA5* for 5′-TGTTCAACCAATTATCAGCAAACTC-3′, rev 5′-TTCTGCTGTATCCTCTTCACCAGT-3′; human *PDIA4* for 5′-CAAGTGTGGGTACGCCACG-3′, rev 5′-AAAGAAGCTCTCCATCCGGTC-3′; mouse *Hsf1* for 5′-AAACTGGCCCTGGTCAAAC-3′; mouse *Hsp90ab1* for 5′-ATCAACTGGGCAATTTCTGC-3′, rev 5′-GTCCTGTGCGGTCACTTAGC-3′; mouse *Hspa8* for 5′-AGCACATTCCTTTCAGCTCC-3′, rev 5′-ATGCTGGAACTATTGCTGGC-3′; mouse *Hspe1* for 5′-CTGACAGGTTCAATCTCTCCAC-3′, rev 5′-AGGTGGCATTATGCTTCCAG-3′; mouse *Dnaja1* for 5′-CTCCTTCACCGTGGAATGTT-3′, rev 5′-AAAAGCTGCAATGGAAGAAAA-3′; mouse *HSPH1* for 5′-AAGGAGTTCCATATCCAGAAGC-3′, rev 5′-GACTCGCACTTTGACTTTTACTC-3′; mouse *Hes1* for 5′-GGTATTTCCCCAACACGCT-3′, rev 5′-GGCAGACATTCTGGAAATGA-3′.

ChIP and ChIP-seq library preparation

For HSF1 ChIP, 50×10^6 cells were fixed with 1% formaldehyde for 10 min at room temperature and lysed on ice using 5 ml cell lysis buffer (50 mM HEPES-KOH, pH 7.5, 140 mM NaCl, 1 mM EDTA, 10% glycerol, 0.5% NP-40 and 0.25% Triton X-100). After centrifugation (5 min, 1300 rpm) at 4°C, the pellet was resuspended in 5 ml buffer II (10mM Tris-HCl, pH8, 200 mM NaCl, 1 mM EDTA, pH8 and 0.5 mM EGTA). After centrifugation (5 min, 1300 rpm) at 4°C, the pellet was resuspended in 600 ul buffer III (10 mM Tris-HCl, pH8, 100 mM NaCl, 1 mM EDTA, pH8 and 0.5 mM EGTA, 0.1% sodium doxycholate and 0.5% n-lauroylsarcosine) and sonicated at a Bioruptor for 40 min. Triton X-100 was added to a final concentration of 1% and the chromatin preparation was pre-cleared using magnetic beads for 1 h. The HSF1 antibody (Cell Signaling, 4356, 5ug) was coupled to magnetic beads (50ul) for 6 h and subsequently added to the pre-cleared chromatin. The reaction mix was incubated for 16 h. The beads carrying the immune-precipitated chromatin fragments were washed eight times with RIPA buffer (50 mM HEPES-KOH, pH 7.6, 300 mM LiCl, 1 mM EDTA, 1% NP-40 (IGEPAL) and 0.7% sodium deoxycholate) and once with TE, followed by treatment with RNase and proteinase K. The cross-links were reversed, and the DNA was precipitated with ethanol and glycogen. NOTCH1 ChIP was performed as described previously[64]. The following primers were used to test NOTCH1 binding enrichment: *HSF1* for 5′-ATTCCCTCCTTGCTCGAGAT-3′, rev 5′-CACGAGGGTCCACAGCTT-3′; *HES1* for 5′-TGGGGACATGGAACCTAGAG-3′, rev 5′-GCGACCTCTCAGATCACCTC-3′. Libraries were generated as described previously[64], including end repair, A-tailing, adaptor ligation (Illumina TrueSeq system) and PCR amplification of the libraries. AMPure XP beads (Beckman Coulter, A63880) were used for DNA cleaning steps.

Notch1-IC protein purification

Mouse Notch1-IC was N-terminal tagged with a single Flag and Strep-tag and cloned in the MIGR1 retroviral plasmid. This plasmid was either transfected in 293T cells or retrovirally infected in the mouse T-ALL 720 cell line. Transfection and infection was confirmed by FACS analysis for presence of GFP. For each protein purification 20×10^6 293T or 720 cells were used. Cells were lyzed in 5 ml IP lysis buffer (20 mM Tris-HCl (pH 7.5), 150 mM NaCl, 1 mM EDTA, 0.5% Triton X-100, 5% Glycerol) supplemented with protease and phosphatase (10mM NaF/1mM Na_3VO_4) inhibitors. Protein lysates were sonicated (bioruptor) for $10 \times 30''$ with $30''$ pause in between pulses and subsequently cleared by centrifugation for $10'$ at 14,000 rpm. Cleared lysate was incubated with 200 µl Streptactin beads (IBA lifescience) for 3 h. Beads were washed three times with 5 ml lysis buffer. Protein was eluted from the beads using a total of 1 ml Desthiobiotin elution buffer (IBA lifescience) and subsequently incubated with 50 µl Flag-M2-beads (sigma) and incubated for 14 h. Beads were washed three times with 1 ml lysis buffer and resuspended in laemli buffer (4% SDS/120 mM Tris pH 6.8/20% Glycerol). Protein was loaded on SDS-PAGE and analyzed with western blot and coomassie staining. Proteins were digested with trypsin and tandem spectra were collected using an orbitrap mass spectrometer.

RNA-seq library preparation

Whole RNA was extracted from 1–5 × 10^6 T-ALL cells or using the RNeasy kit (QIAGEN) according to the manufacturer's protocol. Libraries were constructed using the KAPA Stranded RNA-Seq kit.

Protein-protein interaction network analysis

Protein interaction network was generated using the STRING database[65]. The interactions network was generated with a required confidence score of 0.15 and "Active interaction sources" based on experiments.

RNA-seq analysis

RNA-seq analysis was performed using lncRNA-screen[66]. Specifically, sequencing reads were aligned to reference genome hg19 using STAR aligner[67] and default parameters. Differential expression analysis was performed using DESeq2[68]. The comparisons tested were: (1) γSI treatment versus DMSO; (2) *HSF1* knockdown versus *Renilla*; (3) *HSF1* knockdown plus γSI treatment versus *HSF1* knockdown; and (4) *HSF1* knockdown plus γSI treatment versus *Renilla*. Genes with FDR<0.1 were considered significantly differentially expressed. Other RNA-seq datasets in this study were also analyzed with the same platform and cut-offs.

Data sources and computational tools

Human assembly version hg19/GRCh37 and ENSEMBL annotation release 69 were used for the RNA-sequencing, ChIP-sequencing and data integration analyses. Bowtie (version 2.2.6)[69] and STAR aligner[67] (in the case of RNA-seq) were used for alignment of sequenced reads. HOMER (version 4.6)[70] were used for ChIP-sequencing peak discovery. The R programming language (version 3.3.0), Bioconductor (version 3.4)[71] and microarray-processing packages were used for microarray analysis. GenomicTools version 2.7.2[72] was used for performing genomic interval mathematical operations, genomic interval annotations and ChIP-seq profile construction.

Microarray analysis

Non-normalized expression data from T-ALL patients and normal T-cells (GSE33469 and GSE33470)[24] were normalized using quantile normalization to eliminate any batch effects. Illumina identifiers were converted to gene names using Bioconductor (version 3.4)[71] and Illumina HumanHT12v4 annotation data (R package version 1.26). Expression values were log-transformed and unpaired Student's *t*-test with Benjamini-Hochberg (BH) correction and cutoff P=0.001 was used to determine statistically significant differences between the T-ALL samples and their normal counterparts. Boxplots and Volcano plots were generated with the untransformed normalized expression values (after quantile normalization), using ggplot2[73] in combination with ggrepel (in the case of Volcano; R package version 0.6.5). Mouse microarray data (GSE46797)[29] were processed with the *affy* Bioconductor package[74]. Annotation of the probes was performed using Affymetrix Mouse Genome 430 2.0 Array annotation data. In the case of T-ALL cell lines data (GSE48046)[24] the analysis was performed as for mouse but using Affymetrix Human Genome U133 Plus 2.0 Array data for

annotation. For heatmaps, the expression values were normalized per row (*z*-score). Heatmaps were generated using R (version 3.3.0).

ChIP-seq analysis

Sequenced reads were aligned using Bowtie (version 2.2.6) (with default parameters, except for −m 1 so as to report only unique alignments) on human assembly version hg19. Bases with mapping quality MAPQ < 30 were discarded. Peak discovery for transcription factors (NOTCH1 and HSF1) was performed with HOMER (version 4.6)[70] using default parameters and the "factor" peak style option, optimized for transcription factors. The motif analysis and peak annotation was also performed using HOMER, with the default settings and the previously identified peaks as input. Histone modification ChIP-seq samples were analyzed using MACS and the following settings: --broad –nomodel –extsize=150 --pvalue=1e–4. Sonicated input was used as a control for peak discovery. HSF1 peaks were characterized based on their genome-wide distribution as: TSS (1 kb TSS-flanking regions of transcript isoforms), Gene Body (peaks falling within the gene body, excluding any overlaps with TSS-flanking regions), Upstream (upstream regions 10 kb-100 kb from the TSS excluding those that overlapped with the aforementioned categories and Intergenic (the rest of the peaks). Venn diagrams showing the common targets of certain transcription factors were plotted using the online tool: http://bioinformatics.psb.ugent.be/webtools/Venn/. Snapshots of genomic areas were created using the Human Epigenome Browser at Washington University[75].

Motif analysis

The raw sequence of the human genome (hg19) was downloaded using the UCSC browser and the sequence corresponding to +/− 1kb from the transcription start site (TSS) of genes of interest was extracted. Then, FIMO[76] was used with default settings to search for motifs.

Statistics

For statistical analysis, we used GraphPad Prism software v.7.0c and variance was similar between the groups that were compared. Figure legends specify the statistical analysis used and define error bars. For RNA-seq, ChIP-seq and microarray analysis, the statistical analysis performed is described in the corresponding sections of Methods. The statistical analysis of the intersection of NOTCH1 and HSF1 targets was performed using the SuperExactTest R package (version 0.99.4)[77].

GO analysis

Gene ontology (GO) analysis was performed on the basis of ChIP-seq data and using DAVID v6.8 [78]. The top significantly enriched GO terms were selected for plotting.

GRO-seq analysis

GRO-seq analysis was performed as previously described[79].

Data availability

The data sets generated for this study can be accessed at GEO (GSE90717). Previously published data sets that were re-analyzed during this study include microarray data from T-ALL patients and normal T-cells (GSE33469 and GSE33470)[24], AML (GSE30029)[46], CLL (GSE66117), human T-ALL cell lines (GSE48046)[24], mouse microarray data (GSE46797)[29] and ChIP-seq data for CUTLL1 cells (GSE51800)[80]. Uncropped immunoblots are available in Supplementary Figure 11. A Life Sciences Reporting Summary for this paper is available.

Supplementary Material

Refer to Web version on PubMed Central for supplementary material.

Acknowledgments

We thank all members of the Aifantis laboratory for discussions throughout the duration of this project; T. Papagiannakopoulos and P. Ntziachristos for critical assessment of this work; E. Christians (UPMC Univ. Paris 06, CNRS) for the Hsf1$^{f/f}$ mice; A. Heguy and the NYU Genome Technology Center (supported in part by National Institutes of Health (NIH)/National Cancer Institute (NCI) grant P30CA016087-30) for expertise with sequencing experiments; the NYU Histology Core (5P30CA16087-31) for assistance; C. Loomis and L. Chiriboga for immunohistochemistry experiments; C. Jamieson (UCSD) for human LICs; The ECOG-ACRIN Cancer Research Group for clinical specimens. This work has used computing resources at the High Performance Computing Facility at the NYU Medical Center. A.T. is supported by a Research Scholar Grant (RSG-15-189-01 – RMC) from the American Cancer Society and a Leukemia & Lymphoma Society New Idea Award (8007-17). I.A. is supported by the NIH (R01CA133379, R01CA105129, R01CA149655, 5R01CA173636, 1R01CA194923) and the NYSTEM program of the New York State Health Department (NYSTEM-N11G-255). J.M. was supported by KWF BUIT2012-5358. N.K is supported by a Human Frontiers Science Program (HFSP) Long Term Fellowship (LT000150/2013-L) and previously by a Charles H. Revson Senior Fellowship in Biomedical Science (15-31) and a European Molecular Biology Organization (EMBO) Long Term Fellowship (ALTF 850-2012).

References

1. Dai C, Whitesell L, Rogers AB, Lindquist S. Heat shock factor 1 is a powerful multifaceted modifier of carcinogenesis. Cell. 2007; 130:1005–1018. [PubMed: 17889646]
2. Mendillo ML, et al. HSF1 drives a transcriptional program distinct from heat shock to support highly malignant human cancers. Cell. 2012; 150:549–562. [PubMed: 22863008]
3. Santagata S, et al. Tight coordination of protein translation and HSF1 activation supports the anabolic malignant state. Science. 2013; 341:1238303. [PubMed: 23869022]
4. Xi C, Hu Y, Buckhaults P, Moskophidis D, Mivechi NF. Heat shock factor Hsf1 cooperates with ErbB2 (Her2/Neu) protein to promote mammary tumorigenesis and metastasis. The Journal of biological chemistry. 2012; 287:35646–35657. [PubMed: 22847003]
5. Akerfelt M, Morimoto RI, Sistonen L. Heat shock factors: integrators of cell stress, development and lifespan. Nature reviews. Molecular cell biology. 2010; 11:545–555. [PubMed: 20628411]
6. Dai C. The heat-shock, or HSF1-mediated proteotoxic stress, response in cancer: from proteomic stability to oncogenesis. Philos Trans R Soc Lond B Biol Sci. 2018; 373
7. Gomez-Pastor R, et al. Abnormal degradation of the neuronal stress-protective transcription factor HSF1 in Huntington's disease. Nature communications. 2017; 8:14405.
8. Li J, Labbadia J, Morimoto RI. Rethinking HSF1 in Stress, Development, and Organismal Health. Trends Cell Biol. 2017
9. Luo J, Solimini NL, Elledge SJ. Principles of cancer therapy: oncogene and non-oncogene addiction. Cell. 2009; 136:823–837. [PubMed: 19269363]
10. Nagel R, Semenova EA, Berns A. Drugging the addict: non-oncogene addiction as a target for cancer therapy. EMBO Rep. 2016; 17:1516–1531. [PubMed: 27702988]
11. Gomez-Pastor R, Burchfiel ET, Thiele DJ. Regulation of heat shock transcription factors and their roles in physiology and disease. Nature reviews. Molecular cell biology. 2017

12. Whitesell L, Lindquist S. Inhibiting the transcription factor HSF1 as an anticancer strategy. Expert opinion on therapeutic targets. 2009; 13:469–478. [PubMed: 19335068]
13. Belver L, Ferrando A. The genetics and mechanisms of T cell acute lymphoblastic leukaemia. Nature reviews. Cancer. 2016; 16:494–507. [PubMed: 27451956]
14. Palomero T, et al. NOTCH1 directly regulates c-MYC and activates a feed-forward-loop transcriptional network promoting leukemic cell growth. Proceedings of the National Academy of Sciences of the United States of America. 2006; 103:18261–18266. [PubMed: 17114293]
15. Weng AP, et al. c-Myc is an important direct target of Notch1 in T-cell acute lymphoblastic leukemia/lymphoma. Genes & development. 2006; 20:2096–2109. [PubMed: 16847353]
16. Chou SD, Prince T, Gong J, Calderwood SK. mTOR is essential for the proteotoxic stress response, HSF1 activation and heat shock protein synthesis. PloS one. 2012; 7:e39679. [PubMed: 22768106]
17. Cotto JJ, Kline M, Morimoto RI. Activation of heat shock factor 1 DNA binding precedes stress-induced serine phosphorylation. Evidence for a multistep pathway of regulation. The Journal of biological chemistry. 1996; 271:3355–3358. [PubMed: 8631933]
18. Hietakangas V, et al. PDSM, a motif for phosphorylation-dependent SUMO modification. Proceedings of the National Academy of Sciences of the United States of America. 2006; 103:45–50. [PubMed: 16371476]
19. Holmberg CI, et al. Phosphorylation of serine 230 promotes inducible transcriptional activity of heat shock factor 1. The EMBO journal. 2001; 20:3800–3810. [PubMed: 11447121]
20. Hu Y, Mivechi NF. Promotion of heat shock factor Hsf1 degradation via adaptor protein filamin A-interacting protein 1-like (FILIP-1L). The Journal of biological chemistry. 2011; 286:31397–31408. [PubMed: 21784850]
21. Kourtis N, et al. FBXW7 modulates cellular stress response and metastatic potential through HSF1 post-translational modification. Nat Cell Biol. 2015; 17:322–332. [PubMed: 25720964]
22. Tang Z, et al. MEK guards proteome stability and inhibits tumor-suppressive amyloidogenesis via HSF1. Cell. 2015; 160:729–744. [PubMed: 25679764]
23. Westerheide SD, Anckar J, Stevens SM Jr, Sistonen L, Morimoto RI. Stress-inducible regulation of heat shock factor 1 by the deacetylase SIRT1. Science. 2009; 323:1063–1066. [PubMed: 19229036]
24. Van Vlierberghe P, et al. ETV6 mutations in early immature human T cell leukemias. The Journal of experimental medicine. 2011; 208:2571–2579. [PubMed: 22162831]
25. Guettouche T, Boellmann F, Lane WS, Voellmy R. Analysis of phosphorylation of human heat shock factor 1 in cells experiencing a stress. BMC Biochem. 2005; 6:4. [PubMed: 15760475]
26. Palomero T, et al. CUTLL1, a novel human T-cell lymphoma cell line with t(7;9) rearrangement, aberrant NOTCH1 activation and high sensitivity to gamma-secretase inhibitors. Leukemia. 2006; 20:1279–1287. [PubMed: 16688224]
27. Brandvold KR, Morimoto RI. The Chemical Biology of Molecular Chaperones--Implications for Modulation of Proteostasis. J Mol Biol. 2015; 427:2931–2947. [PubMed: 26003923]
28. Aster JC, et al. Oncogenic forms of NOTCH1 lacking either the primary binding site for RBP-Jkappa or nuclear localization sequences retain the ability to associate with RBP-Jkappa and activate transcription. The Journal of biological chemistry. 1997; 272:11336–11343. [PubMed: 9111040]
29. King B, et al. The ubiquitin ligase FBXW7 modulates leukemia-initiating cell activity by regulating MYC stability. Cell. 2013; 153:1552–1566. [PubMed: 23791182]
30. O'Neil J, et al. Activating Notch1 mutations in mouse models of T-ALL. Blood. 2006; 107:781–785. [PubMed: 16166587]
31. Roderick JE, et al. c-Myc inhibition prevents leukemia initiation in mice and impairs the growth of relapsed and induction failure pediatric T-ALL cells. Blood. 2014; 123:1040–1050. [PubMed: 24394663]
32. Xiao X, et al. HSF1 is required for extra-embryonic development, postnatal growth and protection during inflammatory responses in mice. The EMBO journal. 1999; 18:5943–5952. [PubMed: 10545106]

33. Xiao H, Lis JT. Germline transformation used to define key features of heat-shock response elements. Science. 1988; 239:1139–1142. [PubMed: 3125608]
34. Scherz-Shouval R, et al. The reprogramming of tumor stroma by HSF1 is a potent enabler of malignancy. Cell. 2014; 158:564–578. [PubMed: 25083868]
35. Taipale M, et al. A quantitative chaperone interaction network reveals the architecture of cellular protein homeostasis pathways. Cell. 2014; 158:434–448. [PubMed: 25036637]
36. Grabher C, von Boehmer H, Look AT. Notch 1 activation in the molecular pathogenesis of T-cell acute lymphoblastic leukaemia. Nature reviews. Cancer. 2006; 6:347–359. [PubMed: 16612405]
37. Weng AP, et al. Activating mutations of NOTCH1 in human T cell acute lymphoblastic leukemia. Science. 2004; 306:269–271. [PubMed: 15472075]
38. Wang H, et al. Genome-wide analysis reveals conserved and divergent features of Notch1/RBPJ binding in human and murine T-lymphoblastic leukemia cells. Proceedings of the National Academy of Sciences of the United States of America. 2011; 108:14908–14913. [PubMed: 21737748]
39. Mahat DB, Salamanca HH, Duarte FM, Danko CG, Lis JT. Mammalian Heat Shock Response and Mechanisms Underlying Its Genome-wide Transcriptional Regulation. Molecular cell. 2016; 62:63–78. [PubMed: 27052732]
40. Solis EJ, et al. Defining the Essential Function of Yeast Hsf1 Reveals a Compact Transcriptional Program for Maintaining Eukaryotic Proteostasis. Molecular cell. 2016; 63:60–71. [PubMed: 27320198]
41. Kopan R, Ilagan MX. The canonical Notch signaling pathway: unfolding the activation mechanism. Cell. 2009; 137:216–233. [PubMed: 19379690]
42. Ben-Bassat H, Shlomai Z, Kohn G, Prokocimer M. Establishment of a human T-acute lymphoblastic leukemia cell line with a (16;20) chromosome translocation. Cancer Genet Cytogenet. 1990; 49:241–248. [PubMed: 2208060]
43. Holmes R, Zuniga-Pflucker JC. The OP9-DL1 system: generation of T-lymphocytes from embryonic or hematopoietic stem cells in vitro. Cold Spring Harb Protoc. 2009; 2009 pdb prot5156.
44. Core LJ, Waterfall JJ, Lis JT. Nascent RNA sequencing reveals widespread pausing and divergent initiation at human promoters. Science. 2008; 322:1845–1848. [PubMed: 19056941]
45. Yatim A, et al. NOTCH1 nuclear interactome reveals key regulators of its transcriptional activity and oncogenic function. Molecular cell. 2012; 48:445–458. [PubMed: 23022380]
46. de Jonge HJ, et al. Gene expression profiling in the leukemic stem cell-enriched CD34+ fraction identifies target genes that predict prognosis in normal karyotype AML. Leukemia. 2011; 25:1825–1833. [PubMed: 21760593]
47. Fabbri G, et al. Analysis of the chronic lymphocytic leukemia coding genome: role of NOTCH1 mutational activation. The Journal of experimental medicine. 2011; 208:1389–1401. [PubMed: 21670202]
48. Rossi D, et al. Mutations of NOTCH1 are an independent predictor of survival in chronic lymphocytic leukemia. Blood. 2012; 119:521–529. [PubMed: 22077063]
49. Klinakis A, et al. A novel tumour-suppressor function for the Notch pathway in myeloid leukaemia. Nature. 2011; 473:230–233. [PubMed: 21562564]
50. Fabbri G, et al. Common nonmutational NOTCH1 activation in chronic lymphocytic leukemia. Proceedings of the National Academy of Sciences of the United States of America. 2017; 114:E2911–E2919. [PubMed: 28314854]
51. Kamal A, et al. A high-affinity conformation of Hsp90 confers tumour selectivity on Hsp90 inhibitors. Nature. 2003; 425:407–410. [PubMed: 14508491]
52. Rodina A, et al. The epichaperome is an integrated chaperome network that facilitates tumour survival. Nature. 2016
53. Akahane K, et al. HSP90 inhibition leads to degradation of the TYK2 kinase and apoptotic cell death in T-cell acute lymphoblastic leukemia. Leukemia. 2016; 30:219–228. [PubMed: 26265185]
54. Shrestha L, Patel HJ, Chiosis G. Chemical Tools to Investigate Mechanisms Associated with HSP90 and HSP70 in Disease. Cell Chem Biol. 2016; 23:158–172. [PubMed: 26933742]

55. Moulick K, et al. Affinity-based proteomics reveal cancer-specific networks coordinated by Hsp90. Nat Chem Biol. 2011; 7:818–826. [PubMed: 21946277]
56. Taldone T, et al. Synthesis of purine-scaffold fluorescent probes for heat shock protein 90 with use in flow cytometry and fluorescence microscopy. Bioorg Med Chem Lett. 2011; 21:5347–5352. [PubMed: 21802945]
57. Herranz D, et al. Metabolic reprogramming induces resistance to anti-NOTCH1 therapies in T cell acute lymphoblastic leukemia. Nature medicine. 2015; 21:1182–1189.
58. Wang Z, et al. Stabilization of Notch1 by the Hsp90 Chaperone is Crucial for T-Cell Leukemogenesis. Clin Cancer Res. 2017; 23:3834–3846. [PubMed: 28143869]
59. Dai C, Sampson SB. HSF1: Guardian of Proteostasis in Cancer. Trends Cell Biol. 2016; 26:17–28. [PubMed: 26597576]
60. Schopf FH, Biebl MM, Buchner J. The HSP90 chaperone machinery. Nature reviews. Molecular cell biology. 2017; 18:345–360. [PubMed: 28429788]
61. Le Masson F, et al. Identification of heat shock factor 1 molecular and cellular targets during embryonic and adult female meiosis. Molecular and cellular biology. 2011; 31:3410–3423. [PubMed: 21690297]
62. Tatarek J, et al. Notch1 inhibition targets the leukemia-initiating cells in a Tal1/Lmo2 mouse model of T-ALL. Blood. 2011; 118:1579–1590. [PubMed: 21670468]
63. Taldone T, et al. Heat shock protein 70 inhibitors. 2. 2,5′-thiodipyrimidines, 5-(phenylthio)pyrimidines, 2-(pyridin-3-ylthio)pyrimidines, and 3-(phenylthio)pyridines as reversible binders to an allosteric site on heat shock protein 70. J Med Chem. 2014; 57:1208–1224. [PubMed: 24548239]
64. Ntziachristos P, et al. Genetic inactivation of the polycomb repressive complex 2 in T cell acute lymphoblastic leukemia. Nature medicine. 2012; 18:298–301.
65. Jensen LJ, et al. STRING 8--a global view on proteins and their functional interactions in 630 organisms. Nucleic acids research. 2009; 37:D412–416. [PubMed: 18940858]
66. Gong Y, et al. lncRNA-screen: an interactive platform for computationally screening long non-coding RNAs in large genomics datasets. BMC Genomics. 2017; 18:434. [PubMed: 28583068]
67. Dobin A, et al. STAR: ultrafast universal RNA-seq aligner. Bioinformatics. 2013; 29:15–21. [PubMed: 23104886]
68. Love MI, Huber W, Anders S. Moderated estimation of fold change and dispersion for RNA-seq data with DESeq2. Genome biology. 2014; 15:550. [PubMed: 25516281]
69. Langmead B, Salzberg SL. Fast gapped-read alignment with Bowtie 2. Nat Methods. 2012; 9:357–359. [PubMed: 22388286]
70. Heinz S, et al. Simple combinations of lineage-determining transcription factors prime cis-regulatory elements required for macrophage and B cell identities. Molecular cell. 2010; 38:576–589. [PubMed: 20513432]
71. Huber W, et al. Orchestrating high-throughput genomic analysis with Bioconductor. Nat Methods. 2015; 12:115–121. [PubMed: 25633503]
72. Tsirigos A, Haiminen N, Bilal E, Utro F. GenomicTools: a computational platform for developing high-throughput analytics in genomics. Bioinformatics. 2012; 28:282–283. [PubMed: 22113082]
73. Wickham H. Ggplot2 : elegant graphics for data analysis. Springer; New York: 2009.
74. Gautier L, Cope L, Bolstad BM, Irizarry RA. affy--analysis of Affymetrix GeneChip data at the probe level. Bioinformatics. 2004; 20:307–315. [PubMed: 14960456]
75. Zhou X, et al. The Human Epigenome Browser at Washington University. Nat Methods. 2011; 8:989–990. [PubMed: 22127213]
76. Grant CE, Bailey TL, Noble WS. FIMO: scanning for occurrences of a given motif. Bioinformatics. 2011; 27:1017–1018. [PubMed: 21330290]
77. Wang M, Zhao Y, Zhang B. Efficient Test and Visualization of Multi-Set Intersections. Sci Rep. 2015; 5:16923. [PubMed: 26603754]
78. Huang da W, Sherman BT, Lempicki RA. Systematic and integrative analysis of large gene lists using DAVID bioinformatics resources. Nat Protoc. 2009; 4:44–57. [PubMed: 19131956]

79. Rahl PB, et al. c-Myc regulates transcriptional pause release. Cell. 2010; 141:432–445. [PubMed: 20434984]

80. Wang H, et al. NOTCH1-RBPJ complexes drive target gene expression through dynamic interactions with superenhancers. Proceedings of the National Academy of Sciences of the United States of America. 2014; 111:705–710. [PubMed: 24374627]

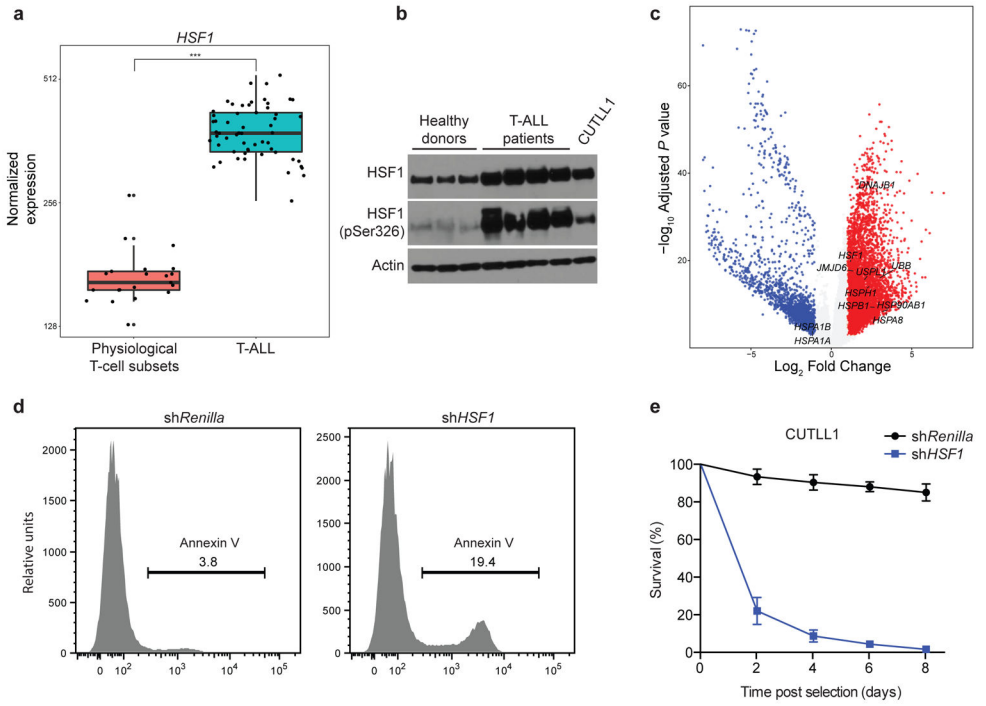

Figure 1. HSF1 and gene-members of the stress response pathway are highly expressed in human T-ALL

a, Box plot showing the expression of *HSF1* among samples of acute T-cell leukemia (T-ALL; n=57 samples) and physiological thymocyte subsets (n=21 samples; 7 T-cell subsets derived from 3 donors)[24] (quantile normalization across samples, see Methods). Boxes represent the first and third quartiles, and the line represents the median. Whiskers represent the upper and lower limits of the range (P=1.7 × 10^{-11}; two-sided Wilcoxon test). ***, significant. **b,** Protein levels of HSF1 (top) and pSer326 HSF1 (bottom) in control T cells ($CD4^+$ T cells) from the peripheral blood of healthy donors, primary bone marrow biopsies from T-ALL patients and the human T-ALL cell line CUTLL1. Representative blots from two independent studies (biological replicates) are shown. **c,** Volcano plot for changes in gene expression in T-ALL patients (n=57 samples) versus physiological thymocyte subsets (n=21 samples; 7 T-cell subsets derived from 3 donors; P<0.001; two-sided unpaired t-test). Red indicates genes expressed higher and blue lower in T-ALL patients versus physiological T-cell subsets. Classic HSF1 targets are depicted. **d,** Annexin V staining upon sh*Renilla* and sh*HSF1* treatment (24 h) of CUTLL1 cells. The experiment was repeated three times (biological replicates) and a representative example is shown. **e,** Effects of *HSF1* or *Renilla* knockdown on human T-ALL (CUTLL1) survival. The mean ± s.d. from three representative studies is shown.

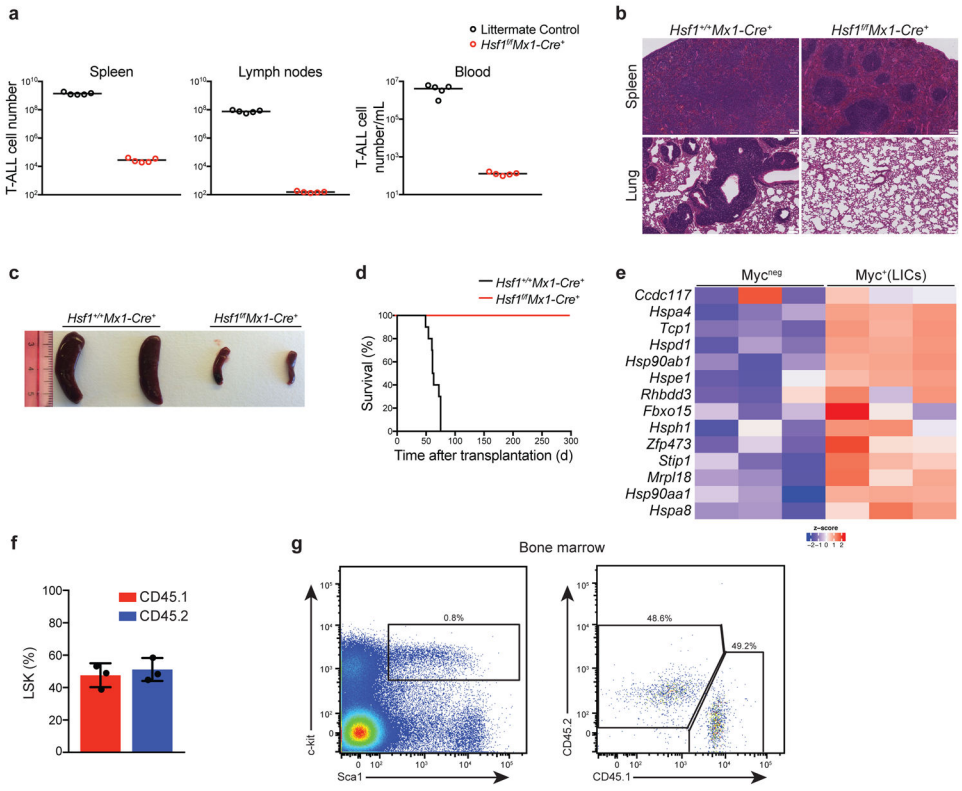

Figure 2. Genetic targeting of *Hsf1* leads to eradication of established T-ALL *in vivo*

a, Number of GFP$^+$ *Hsf1*$^{f/f}$*Mx1-Cre*$^+$ or littermate control (*Hsf1*$^{+/+}$*Mx1-Cre*$^+$) T-ALL cells in the indicated tissues, one month after treatment with poly(I:C) (initiated after GFP$^+$ cells represented ~10% of peripheral blood lymphocytes). Bars represent mean (n=5 per group). **b,** Histology of spleen and lung from *Hsf1*$^{f/f}$*Mx1-Cre*$^+$ or control animals. Representative images from *Hsf1*$^{+/+}$*Mx1-Cre*$^+$ (n=5) and *Hsf1*$^{f/f}$*Mx1-Cre*$^+$ (n=5) mice are shown. Scale bars, 100μm. **c,** Image of representative spleens from *Hsf1*$^{+/+}$*Mx1-Cre*$^+$ (n=5) or *Hsf1*$^{f/f}$*Mx1-Cre*$^+$ (n=5). **d,** Kaplan-Meier survival graph of mice with *Hsf1*$^{f/f}$*Mx1-Cre*$^+$ (n=10) or littermate control (*Hsf1*$^{+/+}$*Mx1-Cre*$^+$, n=10) T-ALL following poly(I:C) treatment (initiated after GFP$^+$ cells represented ~10% of peripheral blood lymphocytes; poly(I:C) injection was defined as day 1). **e,** Heatmap representation of changes in gene expression of mouse homologues of *Hsf1* targets in Myc$^+$ (LICs) versus Myc^{neg} T-ALL cells[29]. **f,** Frequency of CD45.2$^+$ (derived from *Hsf1*$^{f/f}$Mx1-Cre$^+$ animals) competitive donor cells in total Lin$^-$c-kit$^+$Sca-1$^+$ (LSK) bone marrow cells of primary transplanted mice 20-weeks post-reconstitution (mean ± s.d.; n=3 mice per genotype). **g,** Representative flow cytometry of LSKs from the bone marrow of primary transplanted mice (n=3 mice per genotype).

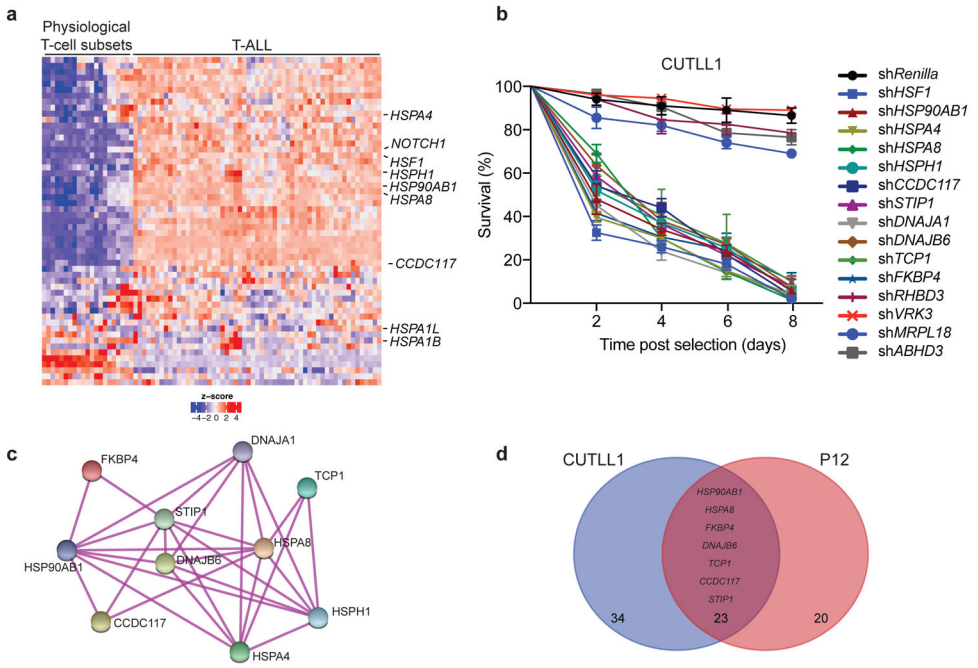

Figure 3. Identification of direct functional HSF1 targets in T-ALL

a, Heatmap representation of changes in gene expression between T-ALL patients and physiological thymocyte subsets (7 thymocyte subsets derived from 3 donors) in all HSF1 promoter-bound genes (±1 kb from TSS). Selected HSF1 targets and NOTCH1 are depicted. **b,** Effects of knockdown of *Renilla*, *HSF1* or HSF1 direct targets (defined as genes bound by HSF1on their promoter and significantly changing expression upon *HSF1* knockdown) on human T-ALL (CUTLL1) survival. Some of the direct HSF1 targets with no effect on T-ALL survival (*FBXO15*, *UBB*, *APTX*, *ZNF473*, *SCNM1*, *MUM1*, *CENPA*, *TRA2B*, *SSBP1*) are omitted for clarity. The mean ± s.d. from three representative studies is shown. **c,** Protein-protein interaction network of HSF1 direct targets mimicking the *HSF1* knockdown effect on T-ALL survival (Fig. 3b; see also Methods). **d,** Venn diagram comparing HSF1 target genes defined by ChIP-seq in CUTLL1 and P12 human T-ALL cell lines. Common HSF1 targets mimicking the *HSF1* knockdown effect on T-ALL survival are indicated.

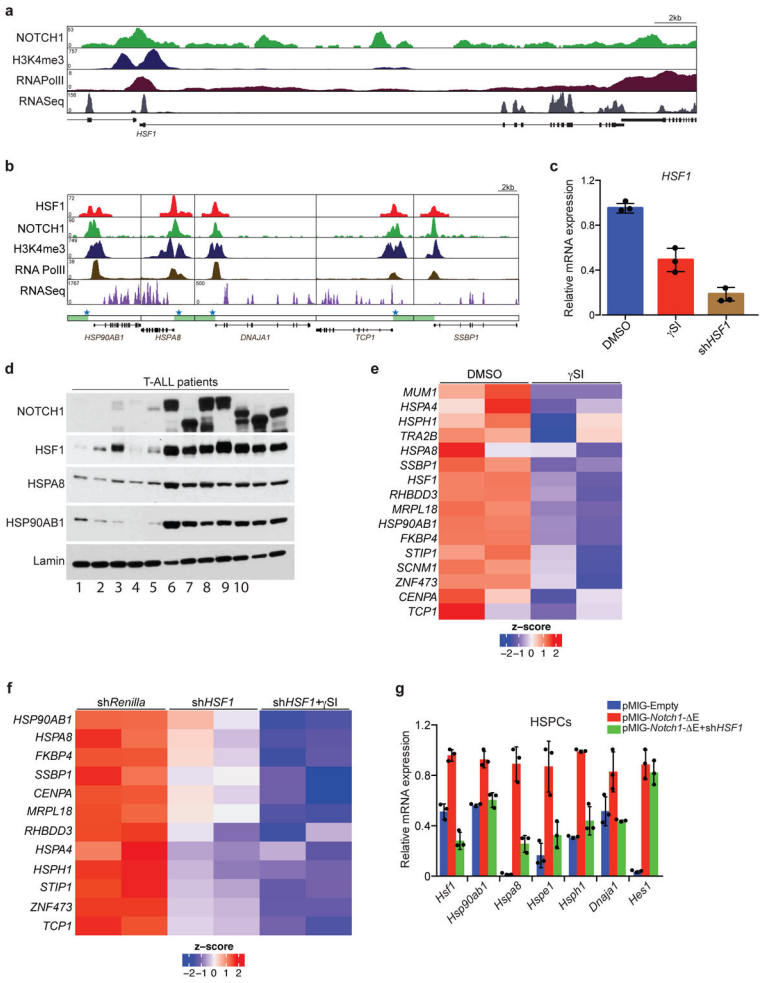

Figure 4. Direct regulation of the heat shock response pathway by NOTCH1

a, Snapshots of NOTCH1 and RNA Pol II binding on *HSF*1 promoter. Enrichment for the histone mark H3K4me3 and expression signal defined by RNA-seq analysis are also indicated. Scale represents reads per million (RPM). Snapshots of common peaks from two independent studies (biological replicates) are shown. **b,** Snapshots of HSF1, NOTCH1 and RNA Pol II binding on the promoters of representative HSF1 targets. Enrichment for the histone mark H3K4me3 and expression signal defined by RNA-seq analysis are also indicated. Scale represents reads per million (RPM). Snapshots of common peaks from two independent studies (biological replicates) are shown. The green region indicates the promoter of the corresponding genes. Asterisks denote the presence of binding motifs for NOTCH1 (RBPJ). **c,** *HSF1* mRNA expression in human T-ALL (CUTLL1) cells upon treatment with γSI or *HSF1* knockdown. The mean ± s.d. from three representative studies is shown. The *P* values (two-sided unpaired *t*-test) are as follows: for DMSO versus γSI, 0.002 and for DMSO versus sh*HSF1* *P*<0.0001. **d,** Protein levels of nuclear NOTCH1, HSF1, HSPA8 and HSP90AB1 from primary bone marrow biopsies of T-ALL patients. Numbered patient samples refer to samples further analyzed in Figure 5 and Supplementary Figure 10. Representative blots from two independent studies (biological replicates) are shown. **e,** Heatmap representation of changes in gene expression of *HSF1* direct targets co-

occupied at the promoter by NOTCH1, upon γSI treatment of human T-ALL (CUTLL1) cells. **f,** Heatmap representation of changes in gene expression of HSF1 direct targets co-occupied at the promoter by NOTCH1, upon *Renilla*, *HSF1* knockdown or combination of γSI and *HSF1* knockdown. Genes that showed cooperative reduction in expression upon combination of γSI and *HSF1* knockdown are shown. **g,** *Hsf1* and HSF1 targets mRNA expression in murine bone marrow hematopoietic stem and progenitor cells (HSPCs) upon overexpression of Notch1-ΔE or overexpression of Notch1-ΔE and downregulation of *HSF1* (*HES1* was used as positive control). mRNA expression was monitored 48h after infection with retrovirus. The mean ± s.d. from three representative studies is shown. For pMIG-Empty versus pMIG-Notch1-ΔE, *P* values (two-sided unpaired *t*-test) are as follows: for *HSF1*, 0.0006; for *HSP90AB1*, 0.0007; for *HSPA8*, 0.0004; for *HSPE1*, 0.0055; for *HSPH1*, $P<0.0001$; for DNAJA1, 0.0498; and for HES1, 0.0002.

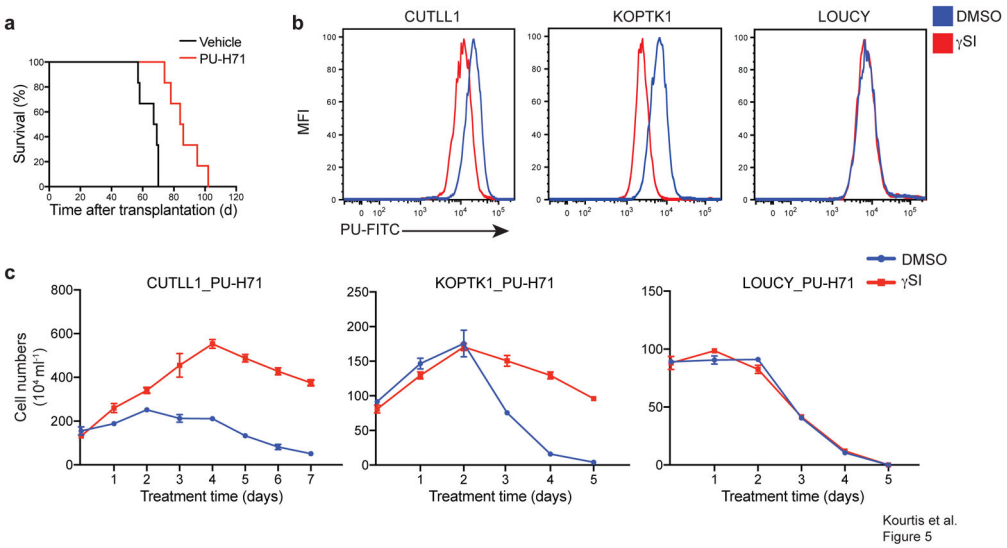

Figure 5. NOTCH1 signaling modulation alters the epichaperome levels

a, Kaplan-Meier survival graph of Notch1-ΔE mice treated with PU-H71 (n=6; 75mg/kg, 3 times per week, intraperitoneally) and vehicle (n=6; Mantel-Cox test; P<0.0008). Treatment was initiated 2 weeks after transplantation, upon detection of ~10% leukemic (GFP^+) cells in the peripheral blood. **b,** Epichaperome abundance measurement as evaluated by binding of fluorescently (FITC) labeled PU-H71 (PU-FITC) in CUTLL1, KOPTK1 and LOUCY T-ALL cell lines upon NOTCH1 inhibition with γSI (1μM) for 24h. Representative plots from three independent studies (biological replicates) are shown. **c,** Cell growth analysis of T-ALL cells (pre-treated with γSI (1μM) or DMSO for 48 h) upon PU-H71 treatment (500nM). The mean ± s.d. from three representative studies is shown.

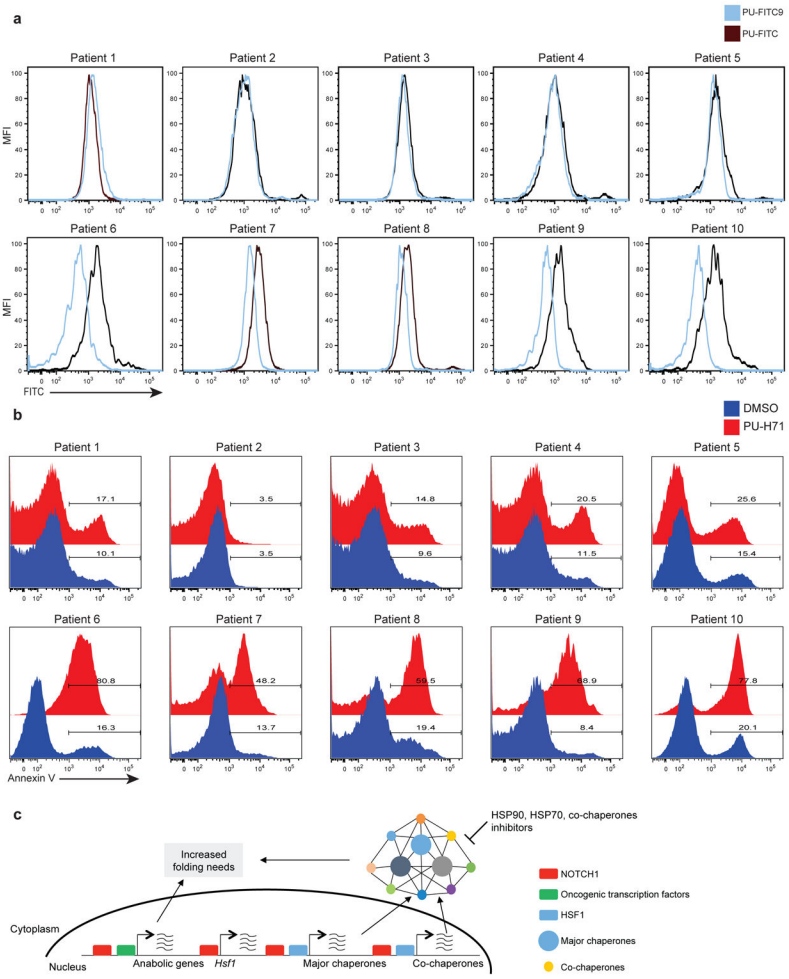

Figure 6. NOTCH1 signaling status correlates with epichaperome levels and predicts response to HSP90 inhibition

a, Epichaperome levels as assessed by binding of PU-FITC in primary T-ALL patient samples. The FITC derivative FITC9 was used as a negative control. **b,** Apoptosis assays using Annexin V staining of primary T-ALL patient samples upon treatment with PU-H71 (500nM) over a period of 48 h. Patient samples numbers correspond to samples in Figure 4d. Representative plots (**a, b**) from three independent studies (biological replicates) are shown. **c,** Model of crosstalk between mediators of oncogene and non-oncogene addiction resulting in a T-ALL vulnerability that can be targeted by inhibitors against HSP90, HSP70 and cancer specific co-chaperones.